Published in final edited form as:
Neurosurgery. 2012 March ; 70(OPERATIVE): ons145–ons156. doi:10.1227/NEU.0b013e31822efcae.

Visual Pathway Study Using *in vivo* DTI Tractography to Complement Classical Anatomy

Wentao Wu, M.D.[1,3,4], **Laura Rigolo, M.A.**[1], **Lauren J. O'Donnell, Ph.D.**[2], **Isaiah Norton, B.S.**[1], **Sargent Shriver, B.S.**[1], and **Alexandra J. Golby, M.D.**[1,2]

[1]Brigham & Women's Hospital, Department of Neurosurgery, Harvard Medical School, Boston, MA, USA

[2]Brigham & Women's Hospital, Department of Radiology, Harvard Medical School, Boston, MA, USA

[3]West China Hospital, Department of Radiology, Sichuan University, Chengdu, Sichuan, China

[4]West China Hospital, Department of Neurosurgery, Sichuan University, Chengdu, Sichuan, China

Abstract

Background—Knowledge of the individual course of the optic radiations (OR) is important to avoid post-operative visual deficits. Cadaveric studies of the visual pathways are limited because it has not been possible to accurately separate the OR from neighboring tracts and results may not apply to individual patients. Diffusion tensor imaging (DTI) studies may be able to demonstrate the relationships between the OR and neighboring fibers *in vivo* in individual subjects.

Objective—To use DTI tractography to study the OR and Meyer's loop (ML) anatomy *in vivo*.

Methods—Ten healthy subjects underwent magnetic resonance imaging with diffusion imaging at 3T. Using a fiducial-based DTI tractography tool (Slicer 3.3), seeds were placed near the lateral geniculate nucleus (LGN) to reconstruct individual visual pathways and neighboring tracts. Projections of the optic radiations onto 3D brain models were shown individually in order to quantify relationships to key landmarks.

Results—Two patterns of visual pathways were found. The OR ran more commonly deep in the whole superior and middle temporal gyri and superior temporal sulcus. The OR was closely surrounded in all cases by an inferior longitudinal fascicle and a parieto/occipito/temporo-pontine fascicle. The mean left and right distances between the tip of the OR and temporal pole were 39.8± 3.8mm and 40.6±5.7 mm, respectively.

Conclusion—DTI tractography provides a practical complementary method to study the OR and ML anatomy *in vivo*, and with reference to individual 3D brain anatomy.

Address for corresponding author: Alexandra J. Golby, M.D. Department of Neurosurgery, Brigham and Women's Hospital, 75 Francis Street, Boston, MA 02115, agolby@bwh.harvard.edu, Telephone: 617-525-6776, Fax: 617-713-3050.

The authors do not hold any significant financial conflict of interest relating to topics of the manuscript.

Funding Disclosure
NIH 1P41RR019703-01A2
NIH P01-CA67165
Brain Science Foundation
Klarman Family Foundation
State Scholarship Fund from China Scholarship Council (CSC)

Keywords

anatomy; DTI tractography; visual pathway; optic radiations; Meyer's loop; white matter

Introduction

The optic radiations(OR) were first identified and described by Louis-Pierre Gratiolet using brain fixation and dissection [1]. Since then, anatomists have displayed the course of the OR using Klingler's fiber dissection technique in cadaveric study [2]. Three bundles of the OR were found in the classic cadaveric study by Meyer, which were named inferior, central, and superior bundles [3]. It is believed that the inferior and superior bundles represent fibers of the lower and upper quadrants of the retina respectively, and the central bundle carries macular information [3,4]. The inferior bundle starts from the lateral geniculate nucleus (LGN), runs in an anterolateral direction into the anterior temporal lobe, rounds the roof of temporal horn (TH) of the lateral ventricle, and loops back to occipital cortex. This loop of the OR is called Meyer's loop (ML) [3]. However, this classical description of the OR has been called into question by recent cadaveric studies [5,6], in which the authors thought it was not possible to accurately delineate the anterior tip of the OR even using micro-dissection techniques in cadaveric studies, particularly amongst a dense network of many neighboring fibers.

Diffusion tensor imaging (DTI) is an MR imaging technique that can be used to characterize the directional properties of the diffusion of water molecules [7]. Application of this technique to the human brain can provide unique *in vivo* visualization of white matter architecture [8]. DTI fiber tractography(DTI-FT) is a mathematical technique to reconstruct white matter tract representations in three-dimensional (3D) space based on DTI. Since DTI-FT offers the only non-invasive method of demonstrating white matter tracts *in vivo*, it may be useful for identifying the OR and ML non-invasively [4,9–13]. However, diffusion tensor fiber tractography for the OR, particularly for ML, is still challenging because tracking algorithms and technique limitations may fail to demonstrate oblique or parallel fiber tracts or tracts with large and/or sharp curvature [9,12,14,15]. Several groups have used DTI tractography to demonstrate the OR and ML and have quantified distances from these structures to the temporal pole, temporal horn and occipital pole [4,15,16]. The results have varied with the largest difference between studies over 20mm. The most powerful validation is comparison of visual field deficits (VFDs) pre- and post-operatively [15,17,18]. Unfortunately, the results even after applying VFD comparison are still quite variable [15,17,18].

The OR are surrounded by numerous neighboring tracts which are not easily dissected from the OR in cadaveric study, especially the anterior part of the OR [5,6]. Little work has specifically described the relationships of the OR, inferior longitudinal fascicle (ILF) and parieto/occipito/temporo-pontine fascicle (POTPF) either in cadaveric or DTI tractography studies [19,20]. Those fascicles are very close to each other, potentially affecting the assessment of location and size of the OR in cadaveric and DTI tractography studies. In addition, no previous work has described the projection of the OR onto a 3D brain surface, within a subject-specific 3D brain model reconstructed from the T1-weighted MR images. Such a model could provide useful information for pre-operative planning. In order to characterize the course and location of the OR and its relationships with other neighboring fascicles, we studied10 healthy subjects.

Methods

Subjects

Ten healthy subjects (three males) without history of neurological disease, head injury, or psychiatric disorder were included (mean age =30±8y). Subjects were recruited after Institutional Review Board approval (Partners Healthcare, Brigham and Women's Hospital, BWH, Boston, MA, USA) and written informed consent was obtained from all subjects.

MRI acquisition

MRI was performed using a 3.0 Telsa machine (GE Sigma, General Electronic, Milwaukee, WI, USA). Whole brain T1-weighted axial 3D-SPGR(spoiled gradient recalled) MR images (TR = 7500ms, TE = 30ms, flip angle = 20°, matrix = 512×512, 176 slices, voxel size = $0.5\times0.5\times1mm^3$) were acquired. A single shot spin-echo echo-planar sequence was used for DTI with diffusion gradients in 31 non-collinear directions (b = 1.000 s/mm^2, matrix = 256×256, 44 slices to cover the whole brain, voxel size = $1\times1\times3mm^3$).

Data processing

DTI computed fractional anisotropy (FA) maps were individually registered with T1-weighted images using Slicer 3.3 (Surgical Planning Laboratory, Brigham and Women's Hospital, Harvard Medical School, Boston, Massachusetts, USA; www.slicer.org). FA maps were displayed as color-orientation FA maps (green: anterior-posterior, red: superior-inferior, blue: left-right). The registration and superimposition of color-orientation FA maps with T1-weighted MR images (anatomic reference) used linear rigid registration suggested by Pataky et al. [21] (Figure 1). This was done by automatically and then manually modifying the linear transformation, such as translation and rotation of FA maps. Then nonlinear transformations, such as inter-slice space resizing of FA maps, were manually modified in Slicer in order to compensate for non-linear deformations inherent in diffusion MRI data [22]. Anatomic precision of the registration was then reviewed by visual analysis of merged images and iterative test-re-test using several landmarks. Landmarks used were: putamen, pallidum, corpus callosum (whole body and/or major and minor forceps), anterior and posterior limbs of the internal capsule, cerebellar contour, tentorium of the posterior fossa, cerebral lobe contour, sylvian regions, upper brainstem contour, ventricular system (frontal horns and trigone), inter hemispheric fissure and several main gyrations (Figure 1). For each subject we generated a 3D brain model and a model of the temporal and occipital horns of the lateral ventricle based on the individual T1-weighted MR images (Figure 2).

Tractography

DTI fiducial-based seeding tractography (continuous diffusion tensor algorithm, [23]) in Slicer was applied. To reconstruct the relevant white matter fascicles, multiple fiducial volumes were seeded along the optic tracts, near the LGN or next to the OR according to anatomical references methods to identify the LGN and optic tracts in T1-weighted images and FA maps as previously described [15,24,25]. The LGN is described as a lenticular-shaped structure with high signal intensity, lateral and caudal to the pulvinar of the thalamus in T1-weighted magnetization-prepared rapid gradient-echo image (13.5/7/2; inversion time, 300ms; matrix, 192×3×256; field-of-view, 200 mm; 48 sections of 72-mm slab thickness [26]). On FA maps, the LGN is a black area medial to the green color region representing fiber tracts that run through temporal stem [24,25]. The optic tracts partially encircle the hypothalamus and the rostral portions of the crus cerebri on T1-weighted images. The multi-colored region (mix of all 3 colors) lateral to the blue and red crus cerebri in FA map also represented the optic tracts [24,25] (Figure 3-A).

DTI fiducial seeding tractography was performed with linear measurement stopping mode and tracking curvature thresholds, respectively, of 0.12–0.15 and 0.4–0.6 degree/mm as suggested by Dauguet et al.'s study [27]. Four white matter fascicles were reconstructed: the optic tract-optic radiation fascicle (OR), Meyer's loop (ML), the fronto-occipital part of the inferior longitudinal fascicle (IFOF), and the parieto/occipito/temporo-pontine fascicle (POTPF). To ensure that reconstructed OR fascicles connected the optic chiasm and occipital lobes through the LGN, fiber tracking was seeded from multiple fiducial volumes (cubic seeder of 0.5mm edge) placed on the optic tracts near LGN. After comparing with the methods and results of classical DTI studies [4,15,16,17,18], we hypothesized that our method should be more accurate than seeding directly in the LGN based on the following three considerations. First, the boundary between the optic tracts and crus cerebri was more obvious than that between the LGN and neighboring tracts, because different color-coded directions of tracts could be easily identified. Second, we could also check whether the OR could pass the LGN and connect the optic chiasm or not, to make sure the tracts reconstructed belong to the visual pathways. Third, in their cadaveric study, Türe and Yasargil also thought the beginning part of OR was amongst a dense network of many neighboring fibers [5,6], so seeding directly in the LGN may increase the possibility of including neighboring tracts.

The number of fiducial volumes did not have a predefined upper limit; rather, fiducials continued to be added until no further expected fibers were found. After the OR was identified, fiducial volumes or seeders for the IFOF were placed lateral to the OR to reconstruct fascicles connecting the frontal lobe and the occipital lobe and next to the OR. Fiducial volumes for the POTPF were placed medial to the OR to reconstruct fascicles connecting the parietal/occipital/temporal lobe and the pons. The number of streamlines of the reconstructed OR was counted in all subjects. A paired t-test was applied to the results comparing left and right OR with a significant difference set at $P<0.05$.

To verify the reproducibility across observers, we involved seven clinicians as raters (two neurosurgeons, two radiologists, two oncologists, and one psychiatrist). They were shown how to use the software and were asked to independently reconstruct the right visual pathway of one healthy subject using our method. The number of streamlines of the reconstructed OR was counted.

Data analysis

Three distances were measured: between the anterior tip of the OR (Tor) and the temporal horn of the lateral ventricle (Tor-TH), Tor and temporal pole (Tor-TP), and between Tor and occipital pole (Tor-OP) (Figure 3-B). These distances were measured parallel to the AC-PC plane and perpendicular to the coronal plane of T1-weighted images. Because of inherent distortion in the FA maps [22] despite co-registration and manual modification of the two images, the T1-weighted images and FA maps still were not exactly aligned. The mesencephalons in T1-weighted images were always a little longer than those in FA maps, so the LGN in T1-weighted images were always a little posterior to those in FA maps. Therefore, we calculated a compensated anterior-posterior distance (Ca-p) between the T1-weghted image and the FA map(Figure 3-C). The Ca-p distances were measured between the posterior edges of the mesencephalon in the T1-weighted images and FA maps. The Tor-TH and Tor-TP were corrected by adding the Ca-p distances, and the Tor-OP were corrected by subtracting the Ca-p distances.

Results

Course of the visual pathways

In all subjects, superior, central and inferior bundles of the visual pathways were identified from the optic chiasm through the LGN to the calcarine sulcus. The OR originated from the LGN, and ran laterally and dorsally along the temporal horn of the lateral ventricle, and laterally along the occipital horn of the lateral ventricle. The OR is most closely approximated to the ventricle at the occipital horn. Two patterns of the visual pathways were found: (1) the ML first extended a small distance in an anterolateral direction before looping back towards the occipital lobe (Figure 4-A) and (2)the ML ran directly towards the occipital lobe without looping (Figure 4-B). The numbers of streamlines of the left reconstructed OR ranged from 15 to 27, mean ± standard deviation 19±4, while that of the right OR ranged from 16 to 28, mean 21±4. The paired t-test on numbers of streamlines of the left and right OR was not significant ($P > 0.05$). The numbers of streamlines of the right reconstructed OR by observers ranged from 21 to 25, mean ± standard deviation 23±1. The variability of morphology among observers can be visualized in Figure 5. All the raters showed the similar second pattern of right visual pathways. The similar morphology of the reconstructed OR and small variability of the numbers demonstrate high reproducibility across observers.

Projection of the OR and ML onto the surface of the 3D brain model

Based on data from the individual 3D brain model reconstruction, the relationships between the OR/ML and temporal gyri and sulci can be described. The OR were found to run more likely deep in the whole superior and middle temporal gyri and superior temporal sulcus, while the ML were more commonly found deep along the inferior part of superior temporal gyrus and superior temporal sulcus. In two subjects, the ML could be seen deep in middle temporal gyrus (Figure 6). The left and right average distances from lateral edge of the OR to brain surface were 33.50±1.07mm and 33.02±0.73mm, respectively (Table 1).

Relationship between the visual pathways, IFOF and POTPF

The visual pathways demonstrated a close relationship with IFOF and POTPF. These tracts were in close proximity crossing one another, but only the visual pathways ran through LGN. It was also found that fewer neighboring tracts mixed with the optic tracts, but much more neighboring tracts mixed with the OR, especially at the beginning part of the OR from the LGN. The relationships of the visual pathways, IFOF and POTPF are shown in Figure 7. The IFOF and POTPF were lateral and medial tracts to the OR, respectively. The left and right average distances from lateral edge of the IFOF to brain surface were 31.05±1.71mm and 31.16±1.19mm, respectively. The left and right average distances from lateral edge of the POTPF to brain surface were 34.94±1.82mm and 35.36±2.28mm, respectively (Table 1).

Distances measured for evaluating the location of OR *in vivo*

The distances measured for evaluating the location of the anterior tip of OR *in vivo* are listed in Table 2. We compared the distances obtained in our study with those obtained in (1) a cadaveric study using Klingler's fiber dissection technique (Ebeling, 1988); (2) patient lesion studies using DTI tractography (Nilsson, 2007, and Yogarajah, 2009); and (3) a patient lesion study using linear regression analysis to estimate the location of the anterior tip of OR (Barton, 2005). The comparisons are also listed in table 2 [2,15,18,28]. The results across studies were inconsistent. The results from Barton's study were consistent with the cadaveric study. However, the tip of the OR in our results was about 13mm posterior to the cadavaric study, the one in Nilsson's results was about 21mm posterior, and the one in Yogarajah's results was about 5mm posterior.

Discussion

This study uses a novel interactive selective tractography method to demonstrate the individual anatomy of the visual pathways in the temporal lobe. After comparing with the methods and results of classical DTI studies [4,15,16,17,18], we hypothesized that our method should be more accurate than seeding directly in the LGN. However, in the future a statistical comparison should be applied between different algorithms to verify the superiority of our method. By serially adding seeder volumes until no further anatomically plausible tracts were found, the proposed method may allow a more exhaustive accounting of the anatomy in this complex small region. Using this approach we were able to demonstrate three bundles of the OR in most patients and two patterns of the visual pathways (Figure 4). The reproducibility of the visual pathway reconstruction was demonstrated to be high by seven clinicians as raters (Figure 5). The first pattern had been described in the classical anatomy of the OR, and the second one was also delineated in a previous cadaveric study. Using reconstructed individual 3D brain models, projection of the OR onto the brain surface could be shown (Figure 6), which could be useful for clinical decision-making such as neurosurgical guidance and planning. We were also able to reveal the relationship between the OR and neighboring tracts (Figure 7), which showed that the IFOF and POTPF were lateral and medial tracts to the OR, respectively.

Two patterns of visual pathways may exist in healthy subjects

Recent cadaveric studies have demonstrated OR and ML with consistent shape and pattern as the classical course of the OR [29,30]. This classical course had also been reconstructed and identified by many investigators using DTI tractography *in vivo* by manually choosing two regions of interest (ROIs) at LGN and calcarine sulcus, respectively [4,15,16]. Based on our results, we hypothesized that two patterns of visual pathways may exist in healthy subjects. The first pattern demonstrated in our study (Figure 4-A) was similar to the classical course. The second pattern seen in our results (Figure 4-B) has also been described in one cadaveric study [5]. The authors of that study concluded “that the classical description of the optic radiation reported by Meyer is incomplete and that further investigation is necessary for an understanding of this complex structure”. Yasargil et al. also thought it was not possible to accurately delineate the anterior tip of the OR, even using micro-dissection techniques in cadaveric studies, particularly amongst a dense network of many neighboring fibers [6]. Although the reproducibility test in our study demonstrated high reliability, due to the technical limitations of the cadaveric study and algorithmic errors of DTI tractography, the real anatomy of the visual pathways still remains unclear, and will need to be investigated in the future research combining cadaveric and DTI tractography results in more subjects.

Significant variability of delineation of the OR exists among healthy subjects and between different studies

In each of the cadaveric and DTI tractography studies, including ours, there are important complexities associated with complete and accurate delineation of the OR and ML. Significant variability was seen not only in each study, but also between different studies. The most significant disparities concerned the average distance from anterior tip of the OR to temporal horn. Distances from different studies varied over 20mm, particularly among DTI studies (Table 2) [2,4,15–18,28–30]. As cadaveric study was still regarded as the gold standard, the findings from Sherbondy et al. seem most accurate because they matched most closely with anatomic results. Nilsson et al. found that VFDs were consistent with DTI tractography changes after they made comparisons between pre- and post-surgery DTI tractography, but the results differed the most from those previously described in anatomic dissection. Many DTI studies used the same two ROIs (LGN and calcarine sulcus), but applied different algorithms for tractography. Chen et al. used the multi-volume of interest

approach (multi-VOIs) at the LGN and occipital cortex and seeding tractography to display the ML pre- and post-operatively in temporal lobe epilepsy surgery in 48 patients. Their results were consistent with gross anatomy findings from cadaveric studies. These various results indicated that DTI tractography of the OR might not be accurate for estimating the location of the OR. However, with the help of individual 3D brain models, the relative location and projection of the OR can be shown individually (Figure 6), which could make the results of DTI tractography more practical and more reliable. The combination of 3D brain modeling and DTI tractography could provide useful guidance for neurosurgeons to estimate resection margins and entry site of surgical approaches.

Our results also suggested that one of the reasons for discrepancies between studies could be the underlying individual significant variability of the OR *in vivo*. Another possible reason might be due to unclear relationships of the OR and neighboring tracts, which can be intermixed and difficult to separate even in cadaveric study [6]. Another reason should be due to the wide variability of measurements, which could be caused by distortion of different measurement modalities in cadaveric and DTI studies, distortion of MRI and DTI images, error of algorithms and so on. Although our reproducibility test showed small variability across observers, it still affected the accuracy of distance measurement.

The classical course of the OR may include many neighboring tracts and the actual size of the OR may be not as large as the classical one

Our results demonstrated that the lateral and medial margins of the OR were the IFOF and POTPF, respectively (Figure 7). One cadaveric study also displayed the relationship between the IFOF and OR [19], but did not mention the relationship between the OR and POTPF. This is likely because it was not possible to separate them, even when applying meticulous microtechniques [6]. We found these tracts were mixed and crossing with each other, and even formed similar loops as ML, which may help to explain why micro-dissection is not able to separate them accurately [6].

The advantages of cadaveric study are that the results are intuitively plausible and, because no co-registration is needed, structural relationships may be clearly observed. The disadvantages are the difficulty in differentiating the real tracts of interest from neigboring tracts due to limitation of dissection techniques [5,6,31]. The potential exists that "demonstrating one fiber tract often resulted in the destruction of another fiber tract" in cadaveric study [6] limit the conclusions which can be inferred from classical gross anatomy of the OR and ML [5,6]. Finally, such an approach could not inform understanding of the individual anatomy *in vivo*. However, the advantages of DTI are the study of individuals *in vivo* and non-invasiveness, but the disadvantages are distortion of FA map, co-registration error, and the inherent calculation error of the tractography algorithm. Distortion of the FA map is related to unfavorable effects of eddy currents [22]. Diffusion tensor images were obtained with echo planar imaging (EPI), which was highly sensitive to eddy currents. The caculation of the diffusion tensors could be impractical if different volumes of the series were distorted relative to each other, and finally resulted in distortion of the FA maps [22]. The distortion of the FA maps leads to misregistration of FA maps relative to the T1-weighted images. Nilsson et al [15] thought classical anatomical "optic radiations" might overestimate the actual size of the OR because they might include part of neighboring tracts, but DTI tractography still might underestimate the actual size of the OR because tracts could be lost or mistakenly reconstructed by mathmatical error of algorithm in LGN.

Using *in-vivo* DTI tractography described in our study, the neighboring tracts could be differentiated from the OR properly because they did not originate from the optic chiasm through LGN to the occipital lobe. Thus, this approach using individualized application of

DTI tractography in individuals could provide complementary information for description of the visual pathways.

Future work regarding anatomical investigation of the visual pathways and its application for pre-surgical planning

The real anatomy of the visual pathways should be verified by cadaveric study because it is still the gold standard. However, so far it is not sufficient, nor is DTI study. Our future work will focus on the development of micro-dissection techniques in cadaveric study and the combination of different algorithms of DTI tractography. One of our aims is to find the real anatomical description of the visual pathways and their neighboring tracts.

Patients with pathological conditions are different from healthy subjects. Another aim in our future work is to use DTI tractography to study the course of the visual pathways in different kinds of patients, and to measure the difference between healthy subjects and patients. This approach has many potential practical surgical applications. Accurate individualized anatomical delineation of the visual pathways and 3D models of brain and lateral ventricle could provide *in-vivo* location, size and edge of optic radiation for pre-surgical planning in patients with tumor, epilepsy, stroke, brain trauma and so on. Neurosurgeons could choose surgical approaches based on this information. In addition, the real-time reconstructed streamlines would be shown in the neuronavigation system by connecting with the Slicer software, so neurosurgeons could accurately evaluate and reduce the deficit of visual functions as much and as early as possible.

Conclusion

The visual pathways are complex structures whose anatomic details remain unclear. Presently, neither cadaveric study nor DTI tractography can fully describe the visual pathways. Although cadaveric study still remains the gold standard to delineate the optic radiations and Meyer's loop, DTI tractography with an individual 3D brain model provides a complementary method to study the OR and ML *in vivo*. In cadaveric study, it is difficult to separate the visual pathways from neighboring tracts and not suitable to apply the results directly to individual patients. Using the *in-vivo* DTI tractography described in our study, the neighboring tracts can be differentiated from the real OR, and the results are directly derived from the data of individual patients, though there remain problems of distortion and algorithm errors. Therefore, by combining the two approaches, it may be possible to balance out the weakness of each approach to produce a more comprehensive and accurate picture of the anatomic configuration of these structures, and apply the results for individual clinic and surgery more reliably.

Acknowledgments

This work was supported by NIH Grants 1P41RR019703-01A2 (National Center for Image Guided Therapy) and P01-CA67165, the Brain Science Foundation, the Klarman Family Foundation, and the State Scholarship Fund (File NO. 2008624048) from China Scholarship Council (CSC). We thank Kun Wang, Jie Duan, Fei Li, Na Hu, Ning He, Jiewei Liu, Tingting Jiang for their work as raters in the reproducibility test.

References

1. Leuret, F.; Gratiolet, L-P. Anatomie comparée du Systéme Nerveux. Vol. II. Paris: J-B Baillére et fils; 1839.
2. Ebeling U, Reulen HJ. Neurosurgical topography of the optic radiation in the temporal lobe. Acta Neurochirurgica. 1988; (92):29–36. [PubMed: 3407471]
3. Meyer A. The connections of the occipital lobes and the present status of the cerebral visual affections. Transactio Association of the American Physicians. 1907; (22):7–23.

4. Yamamoto T, Yamada K, Nishimura T, Kinoshita S. Tractography to depict three layers of visual field trajectories to the calcarine gyri. American Journal of Neuroradiology. 2005; (140):781–785.
5. Türe U, Yaşargil MG, Friedman AH, Al-Mefty O. Fiber Dissection Technique: Lateral Aspect of the Brain. Neurosurgery. 2000; 47(2):417–427. [PubMed: 10942015]
6. Yasargil MG, Türe U, Yasargil DC. Impact of temporal lobe surgery. J Neurosurg. 2004; (101): 725–738. [PubMed: 15540909]
7. Basser PJ, Mattiello J, LeBihan D. MRdiffusion tensor spectroscopy and imaging. Biophys J. 1994; (66):259–267. [PubMed: 8130344]
8. Pierpaoli C, Jezzard P, Basser PJ, Barnett A, Di Chiro G. Diffusion tensor MR imaging of the human brain. Radiology. 1996; (201):637–648. [PubMed: 8939209]
9. Okada T, Miki Y, Kikuta K, Mikuni N, Urayama S, Fushimi Y. Diffusion tensor fiber tractography for arteriovenous malformations: Quantitative analyses to evaluate the corticospinal tract and optic radiation. American Journal of Neuroradiology. 2007; (28):1107–1113. [PubMed: 17569969]
10. Ciccarelli O, Toosy AT, Hickman SJ, et al. Optic radiation changes after optic neuritis detected by tractography-based group mapping. Human Brain Mapping. 2005; (25):308–316. [PubMed: 15834863]
11. Kikuta K, Takagi Y, Nozaki K, et al. Early experience with 3-T magnetic resonance tractography in the surgery of cerebral arteriovenous malformations in and around the visual pathway. Neurosurgery. 2006; (58):331–337. [PubMed: 16462487]
12. Powell HW, Parker GJ, Alexander DC, Symms MR, Boulby PA, Wheeler-Kingshott CA. MR tractography predicts visual field defects following temporal lobe resection. Neurology. 2005; (65):596–599. [PubMed: 16116123]
13. Taoka T, Sakamoto M, Iwasaki S, et al. Diffusion tensor imaging in cases with visual field defect after anterior temporal lobectomy. American Journal of Neuroradiology. 2005; (26):797–803. [PubMed: 15814923]
14. Miller NR. Diffusion tensor imaging of the visual sensory pathway: Are we there yet? American Journal of Ophthalmology. 2005; (140):896–897. [PubMed: 16310467]
15. Nilsson D, Starck G, Ljungberg M, et al. Intersubject variability in the anterior extent of the optic radiation assessed by tractography. Epilepsy Research. 2007; (77):11–16. [PubMed: 17851037]
16. Sherbondy AJ, Dougherty RF, Napel S, Wandell BA. Identifying the human optic radiation using diffusion imaging and fiber tractography. Journal of Vision. 2008; 8(10):12,01–11. [PubMed: 19146354]
17. Chen X, Weigel D, Ganslandt O, Buchfelder M, Nimsky C. Prediction of visual field deficits by diffusion tensor imaging in temporal lobe epilepsy surgery. Neuro Image. 2009; (45):286–297. [PubMed: 19135156]
18. Barton JJ, Hefter R, Chang B, Schomer D, Drislane F. The field defects of anterior temporal lobectomy: a quantitative reassessment of Meyer's loop. Brain. 2005; (128):2123–2133. [PubMed: 15917289]
19. Kier EL, Staib LH, Davis LM, Bronen RA. MR Imaging of the Temporal Stem: Anatomic Dissection Tractography of the Uncinate Fasciculus, Inferior Occipitofrontal Fasciculus, and Meyer's Loop of the Optic Radiation. AJNR Am J Neuroradiol. 2004; (25):677–691. [PubMed: 15140705]
20. Garaci FG, Cozzolino V, Nucci C, et al. Advances in neuroimaging of the visual pathways and their use in glaucoma. Progress in Brain Research. 2008; (173):165–177. [PubMed: 18929108]
21. Pataky TC, Goulermas JY, Crompton RH. A comparison of seven methods of within-subjects rigid-body pedobarographic image registration. J Biomech. 2008; 41(14):3085–3089. [PubMed: 18790481]
22. Yoshikawa T, Aoki S, Abe O, et al. Diffusion tensor imaging of the brain: effects of distortion correction with correspondence to numbers of encoding directions. Radiat Med. 2008; 26(8):481–487. [PubMed: 18975049]
23. Basser PJ, Pajevic S, Pierpaoli C, Duda J, Aldroubi A. In vivo fiber tractography using DT-MRI data. Magnetic Resonance in Medicine. 2000; (44):625–632. [PubMed: 11025519]
24. Niewenhuys, RVJ.; Van Huijzen, C. The Human Central Nervous System. Berlin: Springer-Verlag; 1988.

25. Saeki N, Fujimoto N, Kubota M, Yamaura A. MR demonstration of partial lesions of the lateral geniculate body and its functional intra-nuclear topography. Clin Neurol Neurosurg. 2003; 106(1): 28–32. [PubMed: 14643913]

26. Fujita N, Tanaka H, Takanashi M, et al. Lateral geniculate nucleus: anatomic and functional identification by use of MR imaging. AJNR Am J Neuroradiol. 2001; 22(9):1719–1726. [PubMed: 11673167]

27. Dauguet J, Peled S, Berezovskii V, et al. Comparison of fiber tracts derived from in-vivo DTI tractography with 3D histological neural tract tracer reconstruction on a macaque brain. Neuro Image. 2007; (37):530–538. [PubMed: 17604650]

28. Yogarajah M, Focke NK, Bonelli S, et al. Defining Meyer's loop-temporal lobe resections, visual field deficits and diffusion tensor tractography. Brain. 2009; 132(Pt 6):1656–1668. [PubMed: 19460796]

29. Mahaney KB, Abdulrauf SI. Anatomic Relationship of the optic radiations to the atrium of the lateral ventricle: description of a novel entry point to the trigone. Neurosurgery. 2008; 63:195–203. [PubMed: 18981826]

30. Rubino PA, Rhoton AL Jr, Tong X, Oliveira E. Three-dimensional relationships of the optic radiation. Neurosurgery. 2005; (57):219–227. [PubMed: 16234668]

31. Wang F, Sun T, Li XG, Liu NJ. Diffusion tensor tractography of the temporal stem on the inferior limiting sulcus. J Neurosurg. 2008; (108):775–781. [PubMed: 18377258]

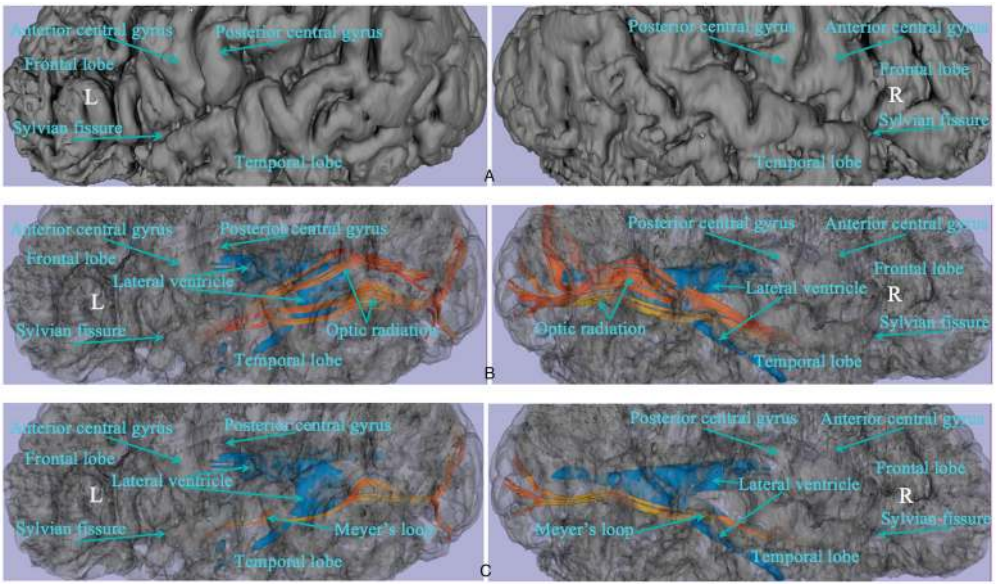

Figure 1.

The first step of co-registration is rigid linear registration and superposition of color-orientation FA maps with T1-weighted MR images. It was done by automatically and then manually modifying linear transformation, such as translation and rotation of the FA maps. The blue ellipse shows the FA maps were still longer and higher than the T1-weighted images after the first step of co-registration. The second step of co-registration is inter-slice space resizing of the FA maps by manually modifying in Slicer to review the anatomic precision of the registration (visual analysis of merged images, iterative test-re-test) using several landmarks: putamen, pallidum, corpus callosum (whole body and/or major and minor forceps), anterior and posterior limbs of the internal capsule, cerebellar contour, tentorium of the posterior fossa, cerebral lobe contour, sylvian regions, upper brainstem contour, ventricular system (frontal horns and trigone), inter hemispheric fissure and several main gyrations.

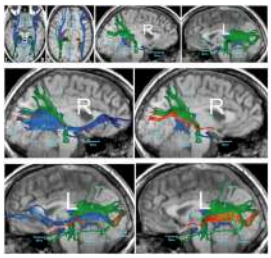

Figure 2.
Individual 3D brain model and model of the temporal and occipital horns of the lateral ventricle based on the individual T1-weighted MR images. The model shows the gyri and sulci of the frontal and temporal lobes and show the projection of the OR and ML onto the cortical surface. The model of lateral ventricle demonstrates its relationship with the nerve fiber bundles reconstructed.

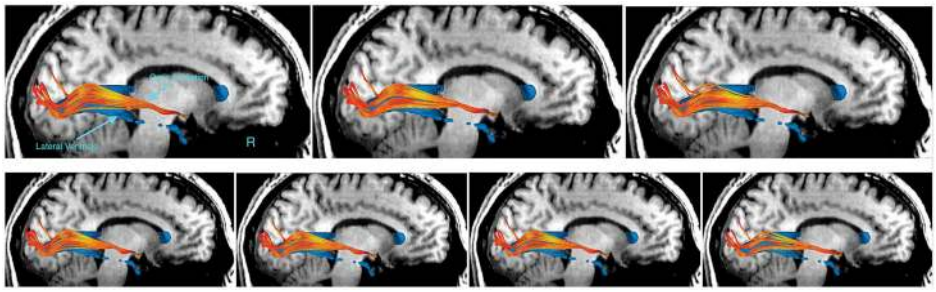

Figure 3.

A) Color-coded axial FA maps demonstrate placement of the fiducial volume seeders for reconstruction of four white matter fascicles of interest. The fiducial volumes were placed in the optic tract near LGN (green indicates fascicles running in an anterior-posterior direction, red superior-inferior, and blue left-right). B) Three distances were measured in every subject: the distances between the anterior tip of the OR (Tor) and the temporal horn of the lateral ventricle (Tor-TH), Tor and temporal pole (Tor-TP), Tor and occipital pole (Tor-OP). Red tracts represent reconstructed visual pathways and blue indicates temporal and occipital horns of the lateral ventricle. C) The compensated anterior-posterior distance (Ca-p)was measured between the posterior edges of mesencephalon of superimposed T1-weighted images (blue image) and FA maps (purple image). LGN: lateral geniculate nucleus; OT: optic tract; OC: optic chiasm

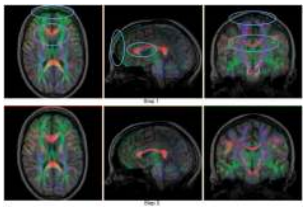

Figure 4.
A) The first pattern of visual pathways in which the tractography demonstrates the ML first extending a small distance in an anterolateral direction before looping back towards the occipital lobe. B) A second pattern of visual pathways in which the tractography demonstrates the ML running directly to occipital lobe without looping. Visual pathways are shown in orange, which include the optic tracts, ML and OR. Individual models of the temporal and occipital horns of the lateral ventricle are shown in blue. Background images are individual T1-weighted axial and sagittal images.

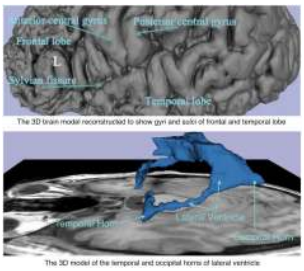

Figure 5.

Reproducibility across observers was verified using seven clinicians as raters. The right visual pathways of the same subject were reconstructed individually and visualized to check the variability. All the raters showed the similar second pattern of right visual pathways, in which the ML ran directly towards the occipital lobe without looping. The ML lied in the bottom part of the OR. The numbers of streamlines of the right reconstructed OR by observers ranged from 21 to 25, mean ± standard deviation 23±1. The similar morphology of the reconstructed OR and small variability of the numbers demonstrate high inter-observer agreement.

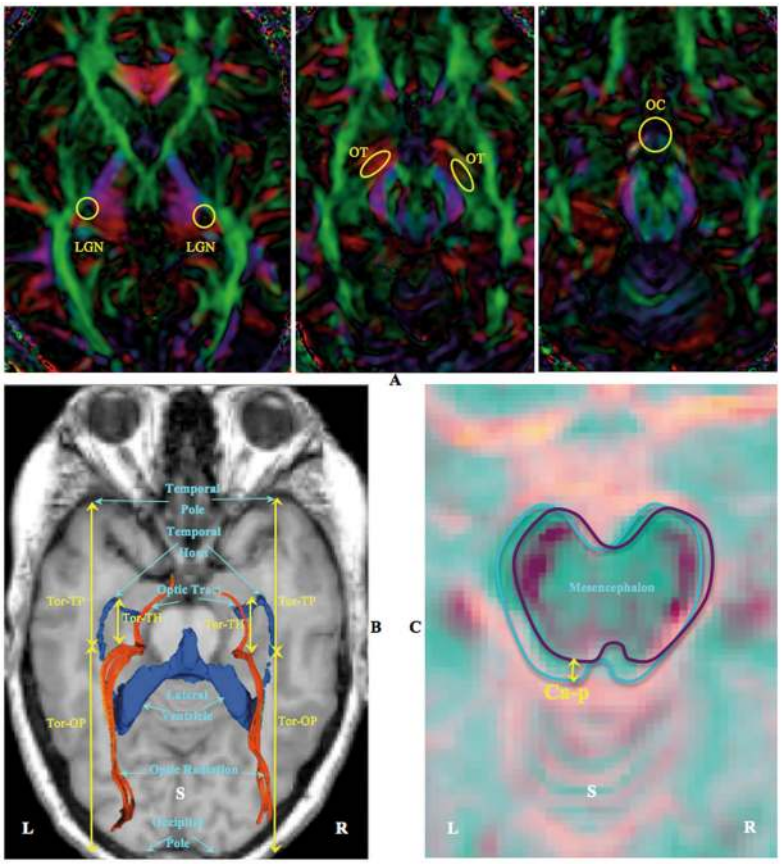

Figure 6.

Individually reconstructed 3D brain model demonstrates projection of the OR and ML onto the brain surface. The OR were found to run deep to the whole superior and middle temporal gyri and superior temporal sulcus, while the ML were found deep along the inferior part of superior temporal gyrus, superior temporal sulcus and middle temporal gyrus. Visual pathways are shown in orange, which include the optic tracts, ML and OR. Individual models of the temporal and occipital horns of the lateral ventricle are shown in blue. Background images are individually reconstructed as the 3D brain model. The opacity degree of brain model ranges from 0 (transparent) to 1 (completely opaque). The opacity in figure A is 1, to best depict the gyral surface. The opacity in B and C is 0.5, to best demonstrate the projection of fiber tracts onto the brain surface.

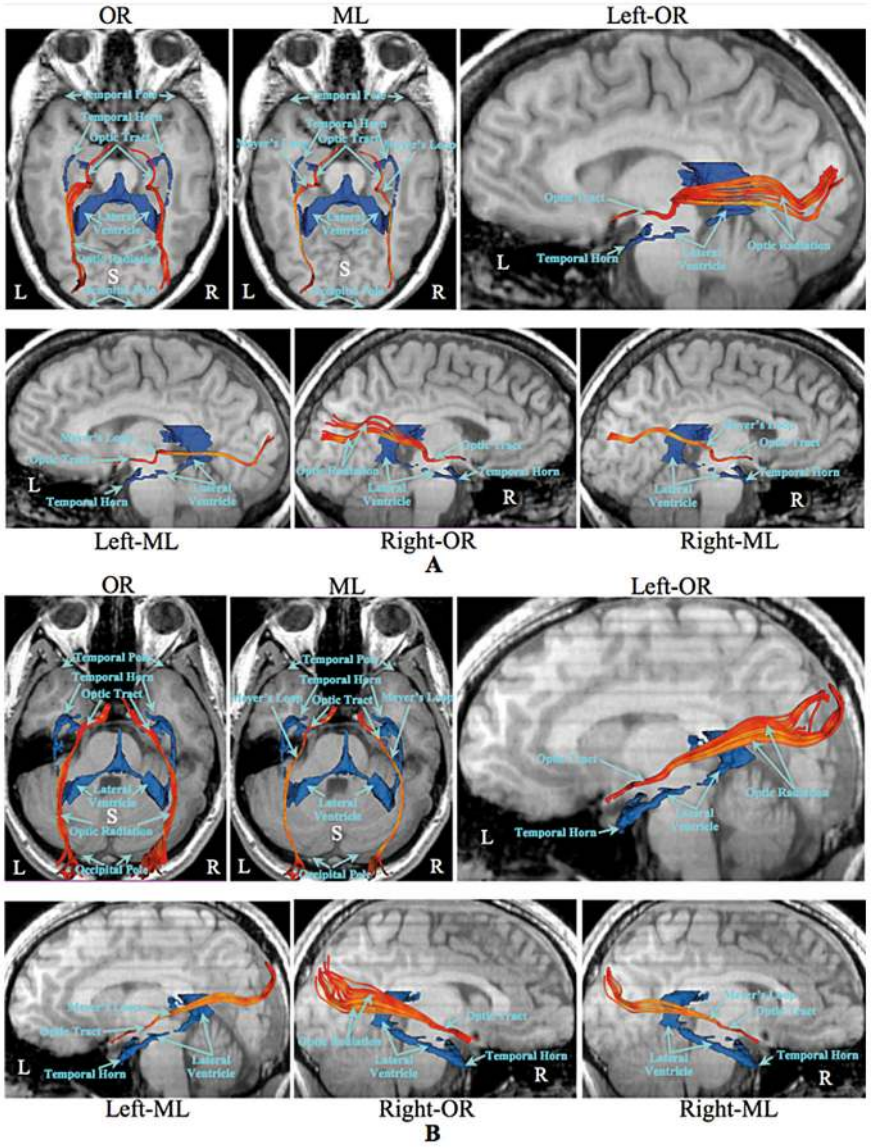

Figure 7.

The relationship among the visual pathways, IFOF and POTPF using DTI tractography demonstrates the IFOF and POTPF are lateral and medial tracts to the OR respectively. Visual pathways are shown in orange, which include the optic tracts, ML and OR. The IFOF and POTPF are shown in blue and green respectively. Individual models of the temporal and occipital horns of the lateral ventricle are shown in blue. Background images are individual T1-weighted axial and sagittal images.

Table 1

The distances from lateral edges of the OR, IFOF, POTPF to the brain surface. The OR is just between the IFOF and POTPF. The IFOF and POTPF are lateral and medial tracts to the OR respectively. LE_{OR} refers to lateral edge of the OR, LE_{IFOF} refers to lateral edge of the IFOF, LE_{POTPF} refers to lateral edge of the POTPF, and BS refers to brain surface.

LE_{OR}-BS (X±SD min-max(mm))		**LE_{IFOF}-BS (X±SD min-max(mm))**		**LE_{POTPF}-BS (X±SD min-max(mm))**	
L	R	L	R	L	R
33.50±1.07	33.02±0.73	31.05±1.71	31.16±1.19	34.94±1.82	35.36±2.28
32.51~35.64	32.04~33.96	29.33~34.72	29.11~33.10	32.97~38.33	33.09~39.30

Table 2

Comparison of distances in cadaveric study using Klingler's fiber dissection technique, patient studies and our study using DTI tractography. The anterior-posterior distances in our study were compensated individually using the compensation distance method described (Ca-p). Posterior is positive relative to the temporal horn (TH) while anterior is negative relative to the temporal horn (TH) in Tor-TH distances.

	Cadaveric study	Patient studies			Present study	
	Ebeling [2], 1988	Nilsson [15], 2007	Yogarajah [28], 2009	Barton [18], 2005	Wentao, 2009	
Measurement	X±SD min-max(mm)	X (mm)	X (mm)	X (mm)	X±SD min-max(mm)	
					L	R
Tor-TH	−5±3.2	16	0		8.69±1.93	9.94±2.63
(distance)	−10~5	8~21	−9~15		7~11.1	6.2~14.7
Tor-TP	27±3.5	44	34		39.86±3.82	40.67±5.74
(distance)	22~37	34~51	24~43	24~28	34.8~49.5	34.6~53.6
Tor-OP	98±6.2				87.19±5.45	85.71±5.38
(distance)	85~108				79.2~95	80.3~94.1